

# Magnetic Resonance Compatibility of Intraocular Lenses Measured at 7 Tesla

Gwyneth A. van Rijn,<sup>1</sup> Jurgen E. M. Mourik,<sup>2</sup> Wouter M. Teeuwisse,<sup>3</sup> Gregorius P. M. Luyten,<sup>1</sup> and Andrew G. Webb<sup>3</sup>

**PURPOSE.** To determine whether intraocular lenses (IOLs) are compatible with magnetic resonance imaging (MRI) at a magnetic field strength of 7 Tesla, the highest field strength at which clinical MRI scans are performed.

**METHODS.** A set of 23 intraocular lenses was selected based on the presence of dyes and metals and different geometric shapes. MR compatibility was evaluated in a high-field 7-Tesla MRI scanner according to the American Standard Test Method (ASTM). The magnetically induced displacement was measured via the angular deflection method. The degree of magnetic susceptibility artifact formation was evaluated by positioning the IOLs in a phantom gel for scanning, using a three-dimensional gradient echo (GRE) sequence. All images were visually inspected to determine the spatial extent of any signal voids. Fiber-optic temperature probes were deployed to measure radio-frequency (RF) heating using a GRE sequence with powers 10 times higher than clinical settings.

**RESULTS.** No significant displacement was detected with any of the tested IOLs. A significant magnetic susceptibility artifact was caused by the small platinum component of the Worst Platinum Clip IOL. None of the other 22 IOLs caused measurable susceptibility artifacts. Measurements on RF-induced heating showed no significant temperature rise (<0.25°C) of the tested IOLs.

**CONCLUSIONS.** MRI did not induce movement or RF heating of any of the IOLs. We conclude that all the tested intraocular lenses are considered safe for MRI up to and including 7 Tesla. One IOL, the Worst Platinum Clip IOL, caused a significant imaging artifact. (*Invest Ophthalmol Vis Sci.* 2012;53:3449-3453) DOI:10.1167/iov.12-9610

**M**agnetic Resonance Imaging (MRI) relies on the principle of nuclear magnetic resonance and involves the patient being placed in a strong static magnetic field, with the image being formed using short pulses of low-frequency (kHz range) magnetic field gradients and high-frequency (hundreds of MHz) radio-frequency (RF) pulses. Clinical MRI scans of the eye are currently performed at a field strength of either 1.5 or 3 Tesla.

With the arrival of higher (7 Tesla) commercial MRI systems, a higher signal-to-noise ratio can be achieved in the image, which can also be utilized for improved spatial resolution. High-resolution, high-field MRI scans may become an important tool for imaging the structures of the eye and retina, since conventional imaging methods like ultrasound imaging, partial coherence interferometry, and optical coherence tomography are limited by optical distortions or depth visualization, and have limited penetration through ocular structures such as the iris and sclera.<sup>1-4</sup> MRI provides depth visualization of the entire eye in any desired anatomic plane. Moreover, MRI does not obstruct binocular vision and enables research of accommodating structures of the eye.<sup>3</sup>

Prior to undergoing an MR examination, every patient should be screened in order to ensure safety and, in a broader sense, confirm that any implants present are MR compatible. The term “MR compatibility” indicates that an object or a device, when used in the MR environment, does not significantly reduce the quality of the diagnostic information via the formation of image artifacts, and that its operation will not be detrimentally affected by the MR device (i.e., it is MR safe). In this sense, safety is defined as the lack of potential injury to the individual and is determined by evaluating whether physical movement or heating of the implant is induced during MR imaging.<sup>5</sup> Knowledge of specific types of implants is essential for screening patients before MRI. All tested implants are considered safe up to a field strength in which they were tested. For higher field systems, all objects and devices should be retested for safety and compatibility prior to screening patients because of the shorter RF wavelengths involved.

Cataract surgery with IOL implantation is the most commonly performed surgery, and incidence is still increasing.<sup>6-8</sup> Because millions of people undergo cataract and refractive surgery with intraocular lens (IOL) implantation worldwide, testing IOLs at a high magnetic field strength MRI is essential in order to warrant the patient's safety. Keizer and Strake tested a selection of IOLs in a magnetic field strength of 1.0 Tesla.<sup>9,10</sup> To our knowledge no testing of IOLs at a field strength of 7 Tesla has been performed.

There are a variety of IOLs on the market, some containing different colors, such as blue-blocking IOLs or IOLs made with colored haptics. In addition, specific older types of IOLs contain metal. The different elements and the composition of an IOL, for example, the presence of dyes or metal, may cause movement and/or heating during an MR procedure. To illustrate the significance, stents, vascular clips, and other implants containing metal elements are being thoroughly tested for MR compatibility as they may be subject to movement or heating.<sup>11</sup> Furthermore, dyes based on iron oxide, as seen in permanent makeup and decorative tattoos, are notorious for causing burning of the skin during an MR procedure.<sup>12-14</sup>

From the <sup>1</sup>Department of Ophthalmology, the <sup>2</sup>Department of Radiology, and the <sup>3</sup>C. J. Gorter Center for High Field MRI, Department of Radiology, Leiden University Medical Center, Leiden, The Netherlands.

Submitted for publication February 1, 2012; revised April 13, 2012; accepted April 16, 2012.

Disclosure: G.A. van Rijn, None; J.E.M. Mourik, None; W.M. Teeuwisse, None; G.P.M. Luyten, None; A.G. Webb, None

Corresponding author: Gwyneth A. van Rijn, Department of Ophthalmology, Leiden University Medical Center, Room J3-235, Albinusdreef 2, 2300 RC Leiden, The Netherlands; g.a.van\_rijn@lumc.nl.

Our hypothesis was that scanning IOLs containing either metal or dyes would cause a higher rise in temperature on or near the IOL due to RF heating, in comparison to clear IOLs. To test this hypothesis, clear and colored IOLs with various geometric shapes, as well as an IOL containing metal, were exposed to a 7-Tesla MR field and examined for magnetically induced movement, heating, and artifact formation. The purpose of this study was to ascertain whether the presence of an IOL, when performing an MR examination at a field strength of 7 Tesla, can influence the image quality or cause damage to the eye as a result of heating or movement.

## METHODS

The IOLs tested were obtained from various manufacturing companies (see Table 2). A set of 23 IOLs was selected, based on the presence of dyes or metal and different geometric shapes. MRI compatibility of the IOLs was evaluated according to American Standard Test Methods (ASTMs) F2052-06 and F2182-09 for magnetically induced displacement and radio frequency-induced heating.<sup>15,16</sup> The formation of magnetic susceptibility-induced image artifacts was also evaluated. MR was performed on an Achieva whole body 7 Tesla MR system (Philips Healthcare, Best, The Netherlands), which is used for clinically related research at Leiden University Medical Center.

### Phantom Formulation

A phantom (gel) was formulated with tissue mimicking conductivity and permittivity for imaging the IOLs and heating tests, according to ASTM protocol. The gel consisted of 1.55 g/L sodium chloride (NaCl) and 31 g/L hydroxyethylcellulose (HEC) in water. To obtain a gel free of air bubbles, suitable for imaging the IOLs, the following procedure was used: A container was positioned in an ultrasound bath. NaCl was added to the water and stirred manually for 20 minutes until completely dissolved. Thereafter, the gel was slowly stirred using an electric stirrer for a period of at least 3 hours until a uniform gel was formed. Finally, the gel was positioned in the 7-Tesla scanner room for at least 24 hours prior to testing, to obtain a transparent gel that was free of bubbles and at room temperature.

### Magnetically Induced Displacement

The magnetically induced displacement was measured via the angular deflection of the IOL, using a protractor mounted on a stand with the zero degree mark at the “6 o'clock position.” The first step was to determine the position along the longitudinal axis of the magnet that gives the maximum deflection angle. To perform this measurement, a slightly ferromagnetic object was hung on a 0.1-mm diameter nylon string. The protractor stand was placed at the center of the patient table in the left-right direction, and the reference position corresponding to maximum deflection was determined by incrementally moving the tabletop into the magnet. Subsequently, the angular deflection from the vertical was measured for all IOLs with the protractor placed at the reference position. During all these measurements, the air circulation in the scanner bore was switched off. In the case where the deflection angle equals 45°, the pulling force exerted by the magnet equals that of gravity. Magnetic forces are considered significant only when the deflection angle is greater than 45°. <sup>15</sup>

### Radio Frequency–Induced Heating

Radio-frequency heating tests were performed with a 6-cm diameter transmit/receive surface coil, which is used for imaging the eye at 7 Tesla. The surface coil is segmented by four equal-value capacitors, to reduce the conservative electric field from the coil. A pi network is used to impedance match the coil to 50 Ω. The IOLs were placed in a small



**FIGURE 1.** For evaluation of radio-frequency heating, IOLs were individually placed in a small chamber. A fiber-optic temperature sensor (Opsens) was positioned as close to the IOL as possible. Temperature was monitored during a multi-slice GRE sequence with high power settings.

chamber formed within an acrylic sheet, which was filled with the formulated gel. An MR-compatible fiber-optic temperature sensor (Opsens, Quebec, Canada) was positioned using a 1-mm-diameter groove, which bisected the chamber so that its tip was positioned within 2 mm of the IOL (Fig. 1). A separate reference measurement, without an IOL present, was performed with the same set-up to determine the temperature rise of the gel itself. The position of the temperature probe was checked prior to and immediately after scanning, for correct and stable positioning. The air circulation was switched off, and the surface coil was placed on top of the chamber, with a 5-mm thick spacer between the chamber and the RF coil. In order to present the “worst case scenario,” the coil was placed off-center with respect to the IOL, so the electric field close to the IOL was at its maximum value. The temperature was monitored during a conventional multi-slice gradient echo (GRE) sequence used for imaging the eye, with power settings above the regulatory clinical scanning parameters. By manipulating the flip angle, repetition time, and allowable maximum RF amplifier, the time-averaged specific absorption rate (SAR) was increased by a factor of 10. This resulted in an averaged SAR of approximately 5 W/kg—well above the value that would be used in any clinical study, which in normal operating mode is limited to 2 W/kg. A period of between 2 and 5 minutes was allowed after placing the set-up in the magnet before temperature data acquisition began in order to allow thermal equilibrium to be established; the criterion for this was a temperature change of no more than 0.1°C over 1 minute. Measurements were performed at least in duplicate per IOL and spread over three sessions. For each session, the test assembly was rebuilt, and a minimum of three reference measurements were taken.

### Evaluation of Image Artifacts

In order to measure any magnetic susceptibility-induced image artifacts, the IOLs were suspended from a nylon string and placed in a box filled with the formulated gel. Image artifacts were evaluated by performing a three-dimensional (3-D) spoiled GRE sequence with TR/repetition time/echo time (TR/TE) = 50/30 ms, flip angle 10°, spatial resolution of 0.22 × 0.22 × 0.22 mm, 105 slices, and field of view 115

TABLE 1. Overview of Results per Group

IOL Group	Temperature Rise	Artifact	
		Formation	Deflection
Clear	0.05°C ± 0.08°C Max 0.18°C	No	<0.5°
Dyed	0.07°C ± 0.07°C Max 0.25°C	No	<1°
Metal	0.07°C ± 0.06°C Max 0.15°C	Yes	<0.5°

× 115 mm. In post-processing, multi-planar reformats were made to reconstruct images parallel and perpendicular to the IOL. All images were visually inspected to determine the presence of any signal voids, and the spatial extent of the voids was determined using the measuring tool as provided by the manufacturer.

RESULTS

An overview of results per group (clear, dyed, and metal-containing IOLs) is shown in Table 1. An overview of individual details for IOL properties and measurement results is shown in Table 2.

The capsular tension ring (Ophtec, Groningen, The Netherlands) was excluded from the deflection tests because the weight of the capsular tension ring was insufficient to pull the string straight down. All other IOLs had sufficiently significant weight to pull the nylon string vertically. A maximum of 1° of deflection was observed during the magnetically induced displacement tests. This is well under the 45° that is considered the threshold for significant deflection. Temperature rises of 0.05°C ± 0.08°C, 0.07°C ± 0.07°C, and 0.07°C ± 0.06°C were observed for the clear, dyed, and metal-containing IOL groups, respectively (Table 1), compared with the control gel. The difference between groups was not statistically significant (ANOVA, P = 0.856). A maximum temperature rise of 0.25°C was measured. The values are essentially identical to that measured in the control gel in the absence of any IOL, suggesting no extra contribution to temperature rise was invoked by the presence of the IOL. The relative mean

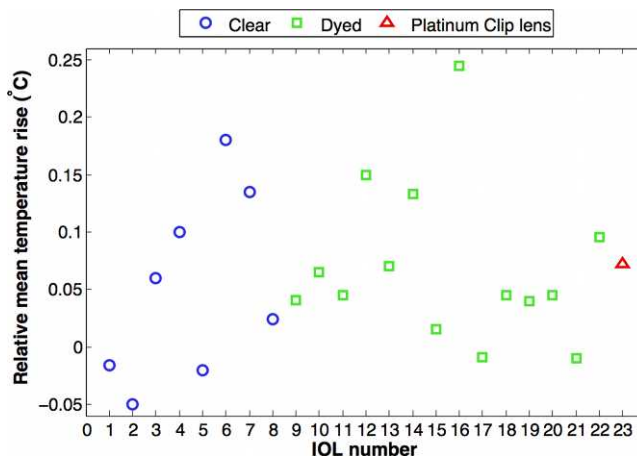


FIGURE 2. Graph showing the relative mean temperature rise per tested IOL. Different colors correspond with clear IOLs (blue), dyed IOLs (green), and a metal-containing IOL (red).

temperature rise of RF heating, per tested IOL, is shown in Figure 2.

A susceptibility artifact of 4 × 5 × 4 mm (width × length × depth) was observed as a signal void at the position of the platinum component of the Worst Platinum Clip IOL (Fig. 3). None of the other 22 IOLs caused measurable susceptibility artifacts (Fig. 4).

DISCUSSION

Various objects used in ophthalmology have been evaluated for safety at various field strengths for safety during an MR procedure.<sup>10,17-22</sup> De Keizer and te Strake tested IOLs at a field strength of 1.0 Tesla.<sup>9</sup> Testing of eyelid implants has been performed at a magnetic field strength of 7 Tesla by Schrom et al.<sup>24</sup> The Ex-PRESS glaucoma shunt has been tested at a field strength of up to 4.7 Tesla.<sup>18</sup> To our knowledge, this is the first

TABLE 2. Overview of All Tested Intraocular Lenses—Properties and Results

IOL Type	Manufacturing Company	Characteristic	Artifact	Deflection	Mean Temperature Rise
Verisyse	Advanced Medical Optics, Santa Ana, CA	Clear	No	0°	0.135
Akreos Adapt AO	Bausch & Lomb, Rochester, NY	Clear	No	<0.5°	-0.016
Microincision Lens MI60	Bausch & Lomb	Clear	No	0°	0.06
Artisan Model 206	Ophtec, Groningen, The Netherlands	Clear	No	0°	-0.02
Capsular tension ring	Ophtec	Clear	No	—	-0.05
Artiflex Model 401	Ophtec	Clear	No	0°	0.024
Quadrimax pc 545	Ophtec	Clear	No	0°	0.1
CT Aspina 409M	Carl Zeiss, Jena, Germany	Clear	No	<0.5°	0.180
Acrysof IQ SN60WF	Alcon, Fort Worth, TX	Dyed	No	0°	0.15
MN60ac 210	Alcon	Dyed	No	<0.5°	0.045
Acrysof MA60 ac 210	Alcon	Dyed	No	<1°	0.245
Z9002	Advanced Medical Optics	Dyed	No	<0.5°	-0.01
ZA9003	Advanced Medical Optics	Dyed	No	0°	0.045
Crystalens HD	Bausch & Lomb	Dyed	No	0°	0.07
AF-1 iMics1 NY60	Hoya Lens, Tokyo, Japan	Dyed	No	0°	0.015
Model 410	Ophtec	Dyed	No	0°	-0.009
Model 430	Ophtec	Dyed	No	<0.5°	0.096
PC-440Y Orange series	Ophtec	Dyed	No	0°	0.04
PC 530 Trimax	Ophtec	Dyed	No	0°	0.133
Lentis LS-312-1Y	Ophtec	Dyed	No	<1°	0.065
C-loop 3 piece L402	Oculentis, Berlin, Germany	Dyed	No	0°	0.045
Lentis LS-313-1Y	Oculentis	Dyed	No	<1°	0.041
Worst Platinum Clip	Ophtec	Metal	Yes	<0.5°	0.07

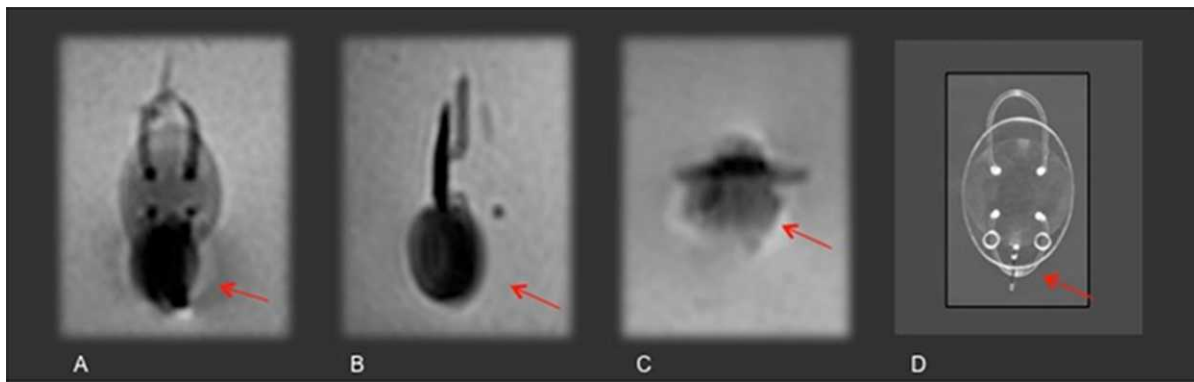


**FIGURE 3.** Reconstructed images showing an artifact around the platinum pin of the Worst Platinum Clip IOL. IOLs were reconstructed in (A) coronal, (B) sagittal, and (C) transverse planes, and visually inspected for signal voids. The *red arrow* indicates an artifact of  $4 \times 5 \times 4$  mm (width  $\times$  length  $\times$  depth). (D) Photograph of Worst Platinum Clip IOL with *red arrow* indicating the platinum component.

time IOLs have been tested at a 7-Tesla magnetic field strength for compatibility during an MR procedure. Testing was done according to ASTM protocol for magnetically induced displacement and radio frequency-induced heating. The formation of magnetic susceptibility-induced image artifacts was also evaluated.

The first safety concern is that an IOL might contain magnetic components, which could experience a force from the static magnetic field (and the gradient in the static magnetic field when the patient is slid into the magnet), which in turn could cause physical movement of the implant and thus damage to the eye. Physical movement of the IOLs was evaluated by measuring the magnetically induced displacement. According to the ASTM standard testing method for magnetically induced displacement, the weight of the nylon string should be no more than 1% of that of the tested devices for the deflection experiment in order for the weight of the string to be considered negligible. In this study, this criterion did not meet strict ASTM standards because of the lightness of the IOLs. We conclude that, within measurement error, there is effectively  $0^\circ$  of deflection, meaning no displacement of the IOLs resulting from the magnetic forces exerted by the static magnetic field. Furthermore, taking into consideration that *in vivo* resistance is provided by ocular tissue, a maximum deflection angle of  $1^\circ$  due to the magnetic field is highly unlikely to result in any movement of the IOLs *in vivo*; thus the risk of displacement caused by the magnetic force is smaller than the risk that is imposed by normal daily activity in the Earth's gravitational field.

During MRI, high-frequency pulses of radio-frequency energy are used to excite the protons. Depending on the

material properties, size, and shape of an implant, an electric current may be formed or (part of) the object or device may act as an antenna, causing heating, which may lead to serious burning of the surrounding tissue.<sup>25</sup> Problems of excessive heating and the induction of electric currents are typically associated with implants that have elongated configurations and/or are electronically activated. Furthermore, the presence of dyes may cause heating, as is seen in metal-based dyes used in tattoos and permanent makeup.<sup>12-14</sup> RF temperature measurements are complex to perform and multi-parameter dependent. Conditions such as room temperature and ventilation, positioning of the test assembly in the bore, and the position of the temperature probe to the IOL were carefully monitored during the study. Nevertheless, five IOLs showed a minimal negative temperature rise compared with the control gel. This can be explained by physiological fluctuations in room temperature and by the complexity and multi-parameter dependence of the measurement method. We measured a maximum temperature rise of  $0.25^\circ\text{C}$  with MR power levels much above regulatory limits. Based on safety standards for MR systems published by the International Electrotechnical Commission (IEC), for healthy subjects with a normal core body temperature of  $37^\circ\text{C}$ , the spatially localized temperature limit of the head is set at  $38^\circ\text{C}$ .<sup>23</sup> This indicates a maximum temperature rise of the head of  $1^\circ\text{C}$  during normal MR operation modes. The maximum temperature increase we observed is well below the value set by the IEC, meaning no safety issues. Furthermore, measurement *in vitro* of temperature rise is likely to overestimate the actual temperature rise for an implant *in situ*, since natural convection in wet tissue will also reduce temperature rise when these conditions are

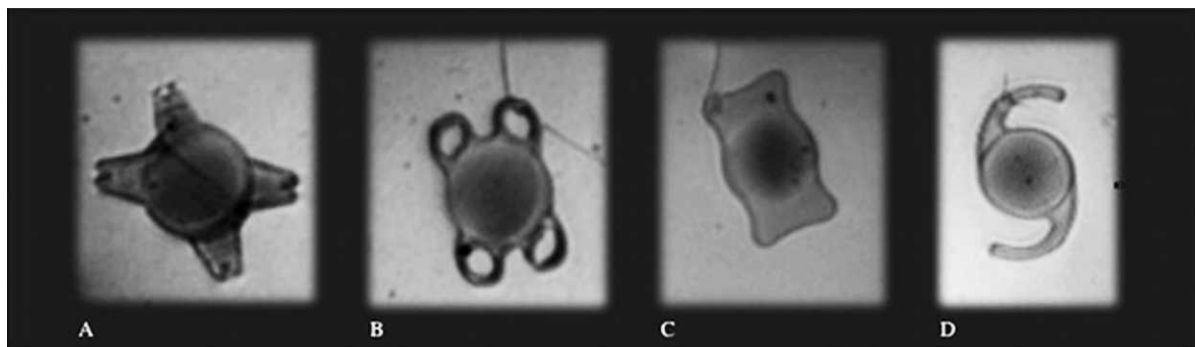


**FIGURE 4.** Examples of reconstructed MR images in coronal plane of (A) Micro Incision Lens (Bausch & Lomb, Rochester, NY), (B) Quadrimax (Ophtec, Groningen, The Netherlands), (C) CT Aspina 409 M (Carl Zeiss, Jena, Germany), and (D) LS 312-1Y (Oculentis, Berlin, Germany). No artifact formation is observed.

present at or near the implant.<sup>16</sup> Between the clear, dyed, and metal-containing IOL groups, no statistical difference in temperature rise was found. Hence, we conclude that there is no additional safety risk for RF heating for the tested dyed and metal-containing IOLs compared with the clear IOLs.

Finally, in order to help clinicians make a decision about the appropriateness of a given MRI scan for a patient with an implant, a statement about image artifact formation of a given object or device should be determined. If an IOL induces a susceptibility artifact, this may lead to diagnostic misinterpretation and/or it may mistakenly be apportioned to pathology if not recognized as such. It is known that platinum can cause low-level susceptibility artifacts.<sup>26</sup> Schrom et al. observed an artifact of platinum-containing eyelid implants.<sup>24</sup> In accordance with their findings, an artifact was observed at the position of the platinum component of the Worst Platinum Clip IOL. Although the artifact we observed around the platinum pin of the Worst Platinum Clip IOL is quite small in terms of size ( $4 \times 5 \times 4$  mm), it would cover a relatively large part of the field of view, hampering 7-Tesla eye imaging. No other IOL showed any measurable image artifact.

In conclusion, all tested IOLs are considered safe for MR imaging at a field strength of up to and including 7 Tesla. Further testing of other surgical materials and implants used in ophthalmology should be performed as well, in order to ensure a patient's safety.

### Acknowledgments

The authors thank the following manufacturers for their donation of a selection of intraocular lenses at no cost: Advanced Medical Optics, Alcon, Bausch & Lomb, Carl Zeiss, Hoya Lens, Oculentis, and Ophtec. Photographs were made by Gerrit Kracht, Department of Radiology, Leiden University Medical Center, The Netherlands.

### References

- Duong TQ, Muir ER. Magnetic resonance imaging of the retina. *Jpn J Ophthalmol*. 2009;53:352-367.
- Strenk SA, Strenk LM, Guo S. Magnetic resonance imaging of aging, accommodating, phakic, and pseudophakic ciliary muscle diameters. *J Cataract Refract Surg*. 2006;32:1792-1798.
- Strenk SA, Strenk LM, Guo S. Magnetic resonance imaging of the anteroposterior position and thickness of the aging, accommodating, phakic, and pseudophakic ciliary muscle. *J Cataract Refract Surg*. 2010;36:235-241.
- Nair G, Tanaka Y, Kim M, et al. MRI reveals differential regulation of retinal and choroidal blood volumes in rat retina. *Neuroimage*. 2011;54:1063-1069.
- Sawyer-Glover AM, Shellock FG. Pre-MRI procedure screening: recommendations and safety considerations for biomedical implants and devices. *J Magn Reson Imaging*. 2000;12:92-106.
- Behndig A, Montan P, Stenevi U, Kugelberg M, Lundström M. One million cataract surgeries: Swedish National Cataract Register 1992-2009. *J Cataract Refract Surg*. 2011;37:1539-1545.
- Congdon N, Vingerling JR, Klein BEK, et al. Prevalence of cataract and pseudophakia/aphakia among adults in the United States. *Arch Ophthalmol*. 2004;122:487-494.
- Erie JC, Baratz KH, Hodge DO, Schleck CD, Burke JP. Incidence of cataract surgery from 1980 through 2004: 25-year population-based study. *J Cataract Refract Surg*. 2007;33:1273-1277.
- de Keizer RJ, te Strake L. Intraocular lens implants (pseudophakoi) and steelwire sutures: a contraindication for MRI? *Doc Ophthalmol*. 1986;61:281-284.
- Shellock FG. MR imaging of metallic implants and materials: a compilation of the literature. *AJR Am J Roentgenol*. 1988;151:811-814.
- Levine GN, Gomes AS, Arai AE, et al. Safety of magnetic resonance imaging in patients with cardiovascular devices: an American Heart Association scientific statement from the Committee on Diagnostic and Interventional Cardiac Catheterization, Council on Clinical Cardiology, and the Council on Cardiovascular Radiology and Intervention: endorsed by the American College of Cardiology Foundation, the North American Society for Cardiac Imaging, and the Society for Cardiovascular Magnetic Resonance. *Circulation*. 2007;116:2878-2891.
- Offret H, Offret M, Labetoulle M, Offret O. Permanent cosmetics and magnetic resonance imaging [in French]. *J Fr Ophtalmol*. 2009;32:131.e1-3. Available at: <http://eutils.ncbi.nlm.nih.gov/entrez/eutils/elink.fcgi?dbfrom=pubmed&id=205794>. Accessed November 14, 2011.
- Morishita Y, Miyati T, Ueda J, et al. Influence of mechanical effect due to MRI-magnet on tattoo seal and eye makeup [in Japanese]. *Nihon Hoshasen Gijutsu Gakkai Zasshi*. 2008;64:587-590.
- Vahlensieck M. Tattoo-related cutaneous inflammation (burn grade I) in a mid-field MR scanner [letter]. *Eur Radiol*. 2000;10:197.
- ASTM Standard F2052-06e1. American Society for Testing of Materials. ASTM International; 2006. Available at: <http://www.astm.org>. Accessed September 14, 2010.
- ASTM Standard F2182-09. American Society for Testing of Materials. ASTM International; 2009. Available at: <http://www.astm.org>. Accessed June 23, 2010.
- Girardot C, Hazebroucq VG, Fery-Lemonnier E, et al. MR imaging and CT of surgical materials currently used in ophthalmology: in vitro and in vivo studies. *Radiology*. 1994;191:433-439.
- Seibold LK, Rorrer RAL, Kahook MY. MRI of the Ex-PRESS stainless steel glaucoma drainage device. *Br J Ophthalmol*. 2011;95:251-254.
- Aksoy FG, Gomori JM, Halpert M. CT and MR imaging of contact lenses and intraocular lens implants. *Comput Med Imaging Graph*. 1999;23:205-208.
- Kuo MD, Hayman LA, Lee AG, Mayo GL, Diaz-Marchan PJ. In vivo CT and MR appearance of prosthetic intraocular lens. *AJNR Am J Neuroradiol*. 1998;19:749-753.
- De Feo F, Roccatagliata L, Bonzano L, et al. Magnetic resonance imaging in patients implanted with Ex-PRESS stainless steel glaucoma drainage microdevice. *Am J Ophthalmol*. 2009;147:907-911, 911.e1. Available at: <http://eutils.ncbi.nlm.nih.gov/entrez/eutils/elink.fcgi?dbfrom=pubmed&id=192325>. Accessed October 26, 2011.
- Marra S, Leonetti JP, Konior RJ, Raslan W. Effect of magnetic resonance imaging on implantable eyelid weights. *Ann Otol Rhinol Laryngol*. 1995;104:448-452.
- IEC 60601-2-33: Medical electrical equipment - Part 2-33: Particular requirements for the basic safety and essential performance of magnetic resonance equipment for medical diagnosis. International Electrotechnical Commission; 2010. Available at: <http://www.iec.ch>. Accessed January 23, 2012.
- Schrom T, Thelen A, Asbach P, Bauknecht H-C. Effect of 7.0 Tesla MRI on upper eyelid implants. *Ophtbal Plast Reconstr Surg*. 2006;22:480-482.
- Schaefer G, Melzer A. Testing methods for MR safety and compatibility of medical devices. *Minim Invasive Ther Allied Technol*. 2006;15:71-75.
- Marshall MW, Teitelbaum GP, Kim HS, Deveikis J. Ferromagnetism and magnetic resonance artifacts of platinum embolization microcoils. *Cardiovasc Intervent Radiol*. 1991;14:163-166.